The Journal of Experimental Biology 207, 1749-1756
Published by The Company of Biologists 2004
doi:10.1242/jeb.00953

Expression and polarity reversal of V-type H^+-ATPase during the mineralization–demineralization cycle in *Porcellio scaber* sternal epithelial cells

Andreas Ziegler[1,*], Dirk Weihrauch[2], Monica Hagedorn[1], David W. Towle[3] and Reiner Bleher[1]

[1]*Central Facility for Electron Microscopy, University of Ulm, Albert-Einstein-Allee 11, 89069 Ulm, Germany*,
[2]*University of Osnabrück, Department of Animal Physiology, Barbarastraße 11, 49076 Osnabrück, Germany* and
[3]*Mount Desert Island Biological Laboratory, Salsbury Cove ME 04672, USA*

*Author for correspondence (e-mail: andreas.ziegler@medizin.uni-ulm.de)

Accepted 18 February 2004

Summary

The formation and resorption of $CaCO_3$ by epithelial cell layers require epithelial transport of protons. We used the anterior sternal epithelium of the terrestrial isopod *Porcellio scaber* as a model to study the expression pattern and immunolocalization of a V-type H^+-ATPase during the mineralization and demineralization of intermittent $CaCO_3$ deposits. Semiquantitative RT-PCR revealed that the expression of the V-type H^+-ATPase increases from non Ca^{2+}-transporting control stages to the stages of $CaCO_3$ deposit formation and resorption. In the Ca^{2+}-transporting stages the expression was larger in the anterior than in the posterior sternal epithelium, which is not involved in deposit formation and transports just moderate amounts of $CaCO_3$. Immunocytochemistry of the B-subunit of the V-type H^+-ATPase in the anterior sternal epithelium reveals an increase in the abundance of the protein within the basolateral membrane, from undetectable to strong signals in the control stage to the stages of $CaCO_3$ deposit formation, respectively. From the stage of $CaCO_3$ deposit formation to that of $CaCO_3$ resorption the signal decreased within the basolateral plasma membrane and increased within the apical plasma membrane. For the first time the results indicate a contribution of a V-type H^+-ATPase to $CaCO_3$ deposition and a reversal of its polarity from the basolateral to the apical plasma membrane compartment within the same cells.

Key words: biomineralization, calcium carbonate, Crustacea, epithelial H^+ transport, epithelium, Isopoda, *Porcellio scaber*.

Introduction

Epithelial proton transport is an important factor in the mineralization and demineralization of calcified tissues that occur during vertebrate bone mineral turnover (Blair et al., 1989) or the formation of shell structures as in molluscs and crustaceans (Cameron, 1989). We used the sternal epithelium of the terrestrial isopod *Porcellio scaber* (Crustacea) as a model to study epithelial H^+-transport during mineral formation and degradation. Isopods molt by shedding first the posterior and then the anterior half of their mineralised cuticle and replace it by a new larger one to allow for growth. About 1 week before the molt, terrestrial species resorb Ca^{2+} and HCO_3^- from the posterior cuticle and store it between the old cuticle of the first four anterior sternites and the anterior sternal epithelium (ASE) as large $CaCO_3$ deposits (Messner, 1965; Steel, 1993). For this to occur, Ca^{2+} and HCO_3^- are transported from the hemolymph across the ASE to form the deposits. Protons that are released during the formation of $CaCO_3$ are then transported in the opposite direction (Fig. 1A). Between the posterior and the anterior molt the sternal $CaCO_3$ deposits are entirely resorbed within less than 24 h and used for the rapid mineralization of the new posterior cuticle to regain full support and protection. Resorption of the deposits requires the transport of protons across the ASE to mobilize Ca^{2+} and HCO_3^- ions, which are then transported into the hemolymph (Fig. 1B). During $CaCO_3$ deposit formation and resorption the ASE is differentiated for ion transport. These differentiations include an increased expression of the plasma membrane Ca^{2+}-ATPase and of the Na^+/Ca^{2+}-exchanger (Ziegler et al., 2002), increased volume density of the mitochondria (Ziegler, 1997b), an increased density of plasma membrane proteins (Ziegler and Merz, 1999), and an increased surface area of the basolateral plasma membrane by a system of ramifying invaginations (Glötzner and Ziegler, 2000). In addition, numerous apical folds enlarge the apical plasma membrane surface area during resorption of the deposits (Glötzner and Ziegler, 2000; Ziegler, 1996). Only minor structural differentiations occur in the posterior sternal epithelium (PSE) of *P. scaber*, which transports just moderate amounts of ions during mineralization and decalcification of the posterior sternal cuticle (Glötzner and Ziegler, 2000; Ziegler, 1997b).

Another interesting aspect of the *P. scaber* model is the

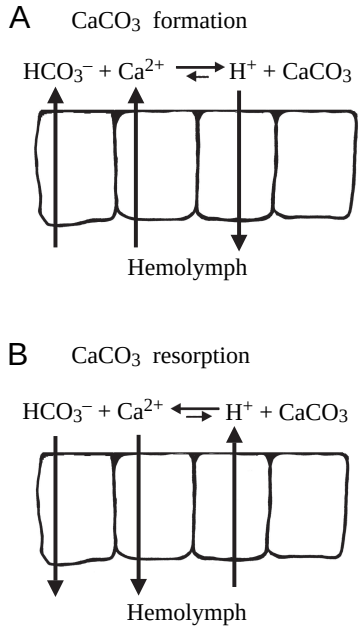

Fig. 1. Schematic representation of the epithelial H^+, Ca^{2+} and HCO_3^- transport during $CaCO_3$ formation (A) and resorption (B).

amorphous character of the sternal deposits (Becker et al., 2002; Ziegler, 1994). Because the solubility of amorphous $CaCO_3$ (ACC) is ten times higher than of its crystalline form (Brecevic and Nielson, 1989), it is ideally suitable as a transient store for Ca^{2+}. Since the solubility product of ACC depends on the pH, the regulation of the H^+ concentration within the limited space around the deposits by epithelial H^+ transport is of particular significance for avoiding $CaCO_3$ crystallisation.

Epithelial proton transport may be mediated by several molecular mechanisms. In crustaceans these include a V-type H^+-ATPase (VHA; Onken and Putzenlechner, 1995; Weihrauch et al., 2001, 2002), a Na^+/H^+-exchanger (Towle et al., 1997) or $2Na^+/H^+$-exchanger, which may also transport one Ca^{2+} in exchange for one H^+ (Ahearn et al., 2001), and a Cl^-/HCO_3^- exchanger (Ahearn et al., 1987). The exact mechanisms for H^+-transport during mineralization processes in Crustaceans, however, are unknown. A recent study has shown an upregulation of the V-type H^+-ATPase activity in crustacean gill epithelia from premolt to the postmolt stage (Zare and Greenaway, 1998), raising the possibility that in the hypodermal epithelium of crustaceans this mechanism contributes to the mineralization and demineralization processes as well.

In an attempt to test a contribution of the VHA to mineral deposition and resorption we analysed the expression of the VHA in the ASE and PSE of *P. scaber* by the reverse-transcriptase polymerase chain-reaction (RT-PCR) technique during three different molting stages and used immunocytochemical and ultrastructural techniques to localize the VHA within the epithelial cells.

Materials and methods

Animals

Isopods *Porcellio scaber* Latr. were kept as described earlier (Ziegler, 1997b). We used *P. scaber* from three different molting stages. Because of their short molt cycle lasting about 6 weeks (Drobne and Strus, 1996) the animals have no defined intermolt stage. Therefore, we used animals 6–8 days after the anterior molt as a control stage. During this early premolt stage the animals have no sternal $CaCO_3$ deposits and, hence, no net calcium transport across the sternal epithelium. Well-developed sternal $CaCO_3$ deposits, which can be seen as white spots at the ventral side of the live animals (Wieser, 1964), defined the late premolt stage in which formation of the deposits takes place. For the stage between the posterior and anterior molt we used animals that had partly degraded $CaCO_3$ deposits to ensure that resorption of the deposits takes place.

Molecular cloning of the V-type H^+-ATPase (VHA) cDNA fragments

We extracted total RNA from sternal tissue of about ten *P. scaber* under RNAse-free conditions using chemicals obtained from Promega Corporation (Madison, WI, USA). Reverse transcription of mRNA was done using oligo (dT) primers and Superscript II (Gibco-BRL, Gaitherberg, MD, USA) reverse transcriptase. We used the degenerate sense primer HATF2: GCN ATG GGN GTN AAY ATG GA and the degenerate antisense primer HATR4: TGN GTD ATR TCR TCG TTN GG (D: A/G/T; N: A/C/G/T; R: A/G; Y: C/T) published previously (Weihrauch et al., 2001) to amplify the putative VHA B-subunit protein fragment of *P. scaber*. PCR products were separated electrophoretically on 1% agarose gels, extracted from gel slices (Qiagen Qiaquick, Valencia, CA, USA) and sequenced automatically by the dideoxynucleotide method (Sanger et al., 1977) at the Marine DNA Sequencing Center of Mount Desert Island Biological Laboratory employing the degenerate PCR primers in the sequencing reactions. A search of GenBank using the BLAST algorithm (Altschul et al., 1997) revealed close matches with previously published sequences for the VHA. For multiple alignments we used Gene Doc (http://www.psc.edu/biomed/genedoc/) and ClustalW (http://antheprot-pbil.ibcp.fr/) software.

Analysis of relative VHE expression

Two independent sets of ASE and PSE were carefully dissected and stored in *RNA*later (Ambion, Austin, TX, USA). For each of the three molting stages within each set we pooled epithelia from 10 animals. After extraction of total RNA we determined the RNA concentration photometrically at 260 nm (Hitachi U2000 ultraviolet-visible spectrophotometer, Tokyo, Japan). Within each set, equal amounts of total RNA were used in either reaction. Semi-quantitative RT-PCR was accomplished by incorporating biotinylated dUTP in the PCR reaction mixture. Amplification proceeded for 27 cycles of 92°C (1 min), 45°C (1 min), and 72°C (1 min) using the degenerated primer pair HATF2 and HATR4 (PCR product size 392 bp). In the logarithmic phase of amplification the

biotinylated products were separated on 1% agarose gels, transferred to nylon membranes and visualized with the PhotoTope detection system (New England Biolabs, Beverly, MA, USA). Under the employed conditions the signal intensity of the PCR product was dependent on the amount of cDNA template (Fig. 3A).

Antibody and western blot analysis of the VHA B-subunit

Sternal epithelia of 24 animals with well-developed sternal $CaCO_3$ deposits were dissected, frozen in liquid nitrogen and stored at –30°C. Lysis buffer (200 µl of 10 mmol l^{-1} Tris containing 0.01% SDS, pH 7.4 and protease inhibitor cocktail, Sigma) was added to the samples, which were then heated to 100°C, homogenized for 3 min using a preheated homogenizer, heated and homogenized for a second round and centrifuged at 16 000 ***g*** for 5 min. The supernatant was diluted 1:1 in 2× SDS loading buffer (Laemmli, 1970). SDS page was done using 10%–20% gradient gels (Novex, Invitrogen, Karlsruhe, Germany). Proteins were electrotransfered overnight onto PVDF-membranes in 10 mmol l^{-1} NaB_4O_7 at 100 mA. The membranes were washed in Tris-buffered saline containing Tween 20 (TBST: 25 mmol l^{-1} Tris-HCl, pH 7.5, 150 mmol l^{-1} NaCl, 0,005% thimerosal, 0.1% Tween 20) for 10 min, blocked in 3% skim-milk in TBST for 1 h, incubated in primary antibody (mouse monoclonal anti yeast VHA B-subunit; Molecular Probes, Leiden, The Netherlands) diluted in 1% skim-milk in TBST at 1:200 for a further 1 h, washed 3× in TBST for 10 min, reacted for 1 h with secondary antibody [horseradish peroxidase (HRP)-coupled anti-mouse IgG; Amersham, Freiburg, Germany] at a dilution of 1:500 in 1% skim-milk in TBST and washed 3× in TBST. Bound antibodies were visualized using a chemiluminescence detection system (ECL, Amersham, Little Chalfont, UK), followed by exposure to Kodak BioMax MS-film.

Immunofluorescence-labelling on cryosections

For the immunofluorescence experiments we fixed the ASE with 4% paraformaldehyde in 0.1 mol l^{-1} cacodylate buffer (pH 7.3) for 1 h. Subsequently, specimens were immersed in 2.3 mol l^{-1} sucrose in 0.1 mol l^{-1} sodium cacodylate buffer for 2 h, mounted on aluminium rods and frozen in liquid nitrogen. Sections (0.7 µm thick) were cut with a Leica Ultracut S microtome (Vienna, Austria) equipped with a FCS cryochamber, glass knives and an antistatic device (Diatome) at –70°C. Sections were transferred to polylysine-coated glass slides (Polyprep, Sigma, Taufkirchen, Germany) with a droplet of 2.3 mol l^{-1} sucrose in 0.1 mol l^{-1} sodium cacodylate buffer. Labelling was done as described previously (Weihrauch et al., 2001). Sections were successively incubated with 0.05 mol l^{-1} glycine in phosphate-buffered saline (PBS) for 15 min, 1% SDS in PBS for 5 min and washed with PBS 3× for 5 min. To block endogenous biotin the sections were incubated with 0.001% streptavidin in PBS for 15 min and washed with PBS for 5 min. Subsequently biotin-binding sites of the streptavidin were blocked by incubation with 0.1% biotin in PBS (15 min). After washing the sections with PBS twice for 5 min, the sections were blocked with blocking solution [3% dry milk and 0.1% cold-water fish gelatine (Biotrend, Cologne, Germany) in PBS] for 15 min. Sections were incubated overnight at 4°C with primary antibody (anti-yeast V-type H^+-ATPase B-subunit) at 2.5 µg ml^{-1} in PBS containing 1% skim-milk. Controls were incubated in the same buffer without the primary antibody. Then the sections were washed 3× with high salt PBS (500 mmol l^{-1} NaCl in PBS) and once with PBS for 5 min each. Subsequently the secondary antiserum, anti-mouse biotinylated IgG (Amersham) diluted 1:100 in 1% milk in PBS was added onto the sections for 1 h. After washing 3× for 5 min with high salt PBS and 5 min with PBS, the sections were treated with blocking solution (TNB: 0.1 mol l^{-1} Tris-HCL, pH 7.5, 150 mmol l^{-1} NaCl, 0.5% blocking reagent; NEN, Boston, MA, USA) for 30 min and incubated with HRP-linked streptavidin (NEN) at a dilution of 1:100 in TNB for 1 h. Sections were washed 3× with high salt PBS and once with PBS for 5 min each. The sections were then incubated with the fluorescent HRP substrate Tyramid-Cy3 (NEN) at a dilution of 1:50 in amplification buffer for 8 min in the dark. After washing 3× for 5 min with high salt PBS and 5 min with PBS the sections were mounted in 80% glycine, 20% PBS plus 2% *N*-propyl-gallate (to retard fading) and examined with a Zeiss Axiophot microscope (Jena, Germany). Micrographs were taken using a Spot CCD camera (Visitron, Puchheim, Germany). The distribution of the basolateral plasma membrane was labeled using the mouse monoclonal anti Na^+/K-ATPase antibody (α5), and FITC-conjugated anti-mouse IgG (Sigma) following the procedure described previously (Ziegler, 1997a).

Electron microscopy

Anterior and posterior sternites from animals in the intermolt, late premolt and intramolt stage were high-pressure frozen at 2.3×10^8 Pa (Leica, EMHPF). Specimens were freeze-substituted in acetone containing 1% OsO_4 and 1% H_2O (Walther and Ziegler, 2002) using a self-built computer-controlled device, following an exponential 24 h warming protocol starting from –90 to 0°C. After incubation for a further 1 h at 0°C in the same solution specimens were washed three times in acetone at room temperature and embedded in Epon resin. For overviews a few samples were chemically fixed as described previously (Ziegler, 1996). Thin sections (60 nm) were cut with a Leica Ultracut UCT microtome using a diamond knife (Diatome), stained with 2% uranyl acetate in H_2O and 0.3% lead citrate, and viewed with a Philips 400 electron microscope at 80 kV.

Results

Expression analysis

Using the degenerate primers for the V-H^+-ATPase (VHA) we amplified a cDNA fragment of 369 nucleotides (GenBank, Accession no. AY278992) from the reverse transcript of the sternal tissue mRNA of *Porcellio scaber*. The deduced partial protein sequence has 100% identity to the known protein

```
PORCELLIO    ---------MEAARFFKQDFEENGSMENVCLFLNLANDPTIERIITPRLALTTAEYLAYQCEKHVLIILTDMSS 65
CALLINECTES  --------------FFKQDFEENGSMENVCLFLNLANDPTIERIITPRLALTTAEYLAYQCEKHVLIILTDMSS 60
MANDUCA      IVFAAMGVNMETARFFKQDFEENGSMENVCLFLNLANDPTIERIITPRLALTAAEFLAYQCEKHVLVILTDMSS 286

PORCELLIO    YAEALREVSAAREEVPGRRGFPGYMYTDLATIYERAGRVEGRQGSITQIPILTMPNDD--------------- 123
CALLINECTES  YAEALREVSAAREEVPGRRGFPGYMYTDLATIYERAGRVEGRQGSITQIPILTMPNDD--------------- 118
MANDUCA      YAEALREVSAAREEVPGRRGFPGYMYTDLATIYERAGRVEGRNGSITQIPILTMPNDDITHPIPDLTGYITEGQ 360
```

Fig. 2. Alignment of *Porcellio scaber* V-type H^+-ATPase B-subunit amino acid fragment sequence (GenBank accession no. AY278992) with the corresponding isoforms of *Callinectes sapidus* (accession no. AF189780) and *Manduca sexta* (accession no. X64354). The black background indicates the agreement between the *Porcellio* and *Callinectes* or *Manduca* sequences.

sequence of the VHA B-subunit of the blue crab *Callinectes sapidus* (GenBank, Accession no. AF 189780) and 96% identity to that of the tobacco hornworm *Manduca sexta* (GenBank, Accession no. X64354) (Fig. 2).

To test if the expression of a VHA is correlated with epithelial Ca^{2+}-transport we analysed the relative expression in sternal epithelia with high (ASE) and moderate (PSE) transport rates in the non-transporting control stage, and the Ca^{2+}-transporting stages during $CaCO_3$ deposit formation and degradation. In two independent experiments the semi-quantitative RT-PCR indicates an increase in VHA expression in both epithelia from the control stage to the Ca^{2+}-transporting stages. In the latter the signal is somewhat larger in the ASE than in the PSE (Fig. 3). The high expression during the formation and resorption of the $CaCO_3$ deposits suggest VHA mediated proton transport in both directions.

Immunocytochemical localization of the VHA

In order to investigate if VHA expression is correlated with a change in the subcellular distribution of the VHE we used a monoclonal antibody to study stage dependent localization of the VHA in the ASE. The antibody against the cytoplasmic B-subunit of the VHA of yeast was successfully used previously to detect the VHA in crustacean gill epithelium (Weihrauch et al., 2001). In western blots of solubilised sternal tissue of *P. scaber* the antibody binds to a single band at an apparent molecular mass of 54 kD (Fig. 4), which is within the range reported for the B-subunit in various eukaryotic cells (for a review, see Finbow and Harrison, 1997), indicating specific binding of the antibody. On cryosections of the ASE location and intensity of the immunoreaction depends on the molting stage. Immunofluorescence was generally weak in the early premolt control stage (Fig. 5A,B). Strong immunofluorescence occurred during the stages of $CaCO_3$ deposit formation and resorption (Fig. 5C,D,G,H). Interestingly, the location of the immunofluorescence changed between the two Ca^{2+}-transporting stages. During $CaCO_3$ deposit formation the antibody binds to some extent to the cuticle of the epithelial cells and to lateral and basal areas (Fig. 5C,D) indicating binding to the basolateral plasma membrane, which forms a system of ramifying invaginations. The nuclei, the cytoplasm around the nuclei, and the cytoplasm between the nuclei and the cuticle were virtually devoid of any signal. The extension of the system of ramifying invaginations is shown by immunocytochemical localization of the Na^+/K^+-ATPase (Fig. 5E,F) and transmission electron microscopy (Fig. 6A). During $CaCO_3$ resorption we observed a strong signal near and within the cuticle. Immunoreaction in the cytoplasm, including basolateral areas and the nuclei, was below the detection limit (Fig. 5G,H). To increase spatial resolution of the strong signal within the cuticle a few sections were stained without an amplification protocol using a Cy3-conjugated donkey anti-mouse IgG as a secondary antibody. These experiments revealed a dot-like distribution of the immunoreaction within the cuticle (Fig. 5I).

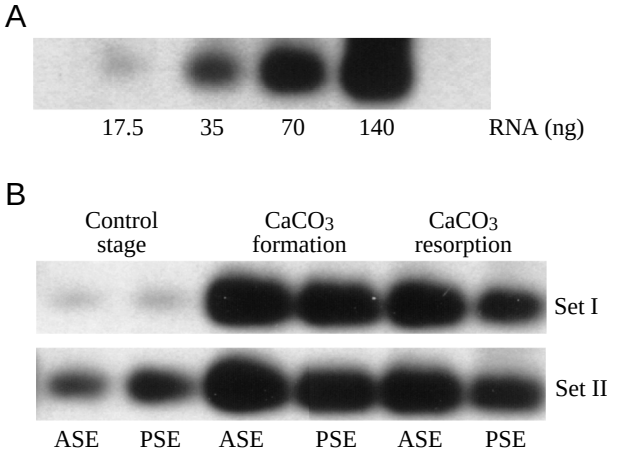

Fig. 3. Semiquantitative RT-PCR analysis of V-type H^+-ATPase (VHA) mRNA abundance in sternal epithelial cells of *Porcellio scaber* during the mineralization–demineralization cycle. (A) Demonstration of template-dependent quantification of VHA B-subunit mRNA. (B) Relative expression of PMCA in the anterior (ASE) and posterior sternal epithelium (PSE).

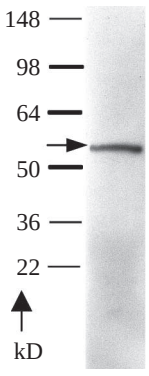

Fig. 4. Western blot analysis of homogenized sternal tissue of *Porcellio scaber*. The monoclonal antibody against the mouse monoclonal anti yeast V-type H^+-ATPase B-subunit protein specifically binds to one band of about 54 kD (arrow).

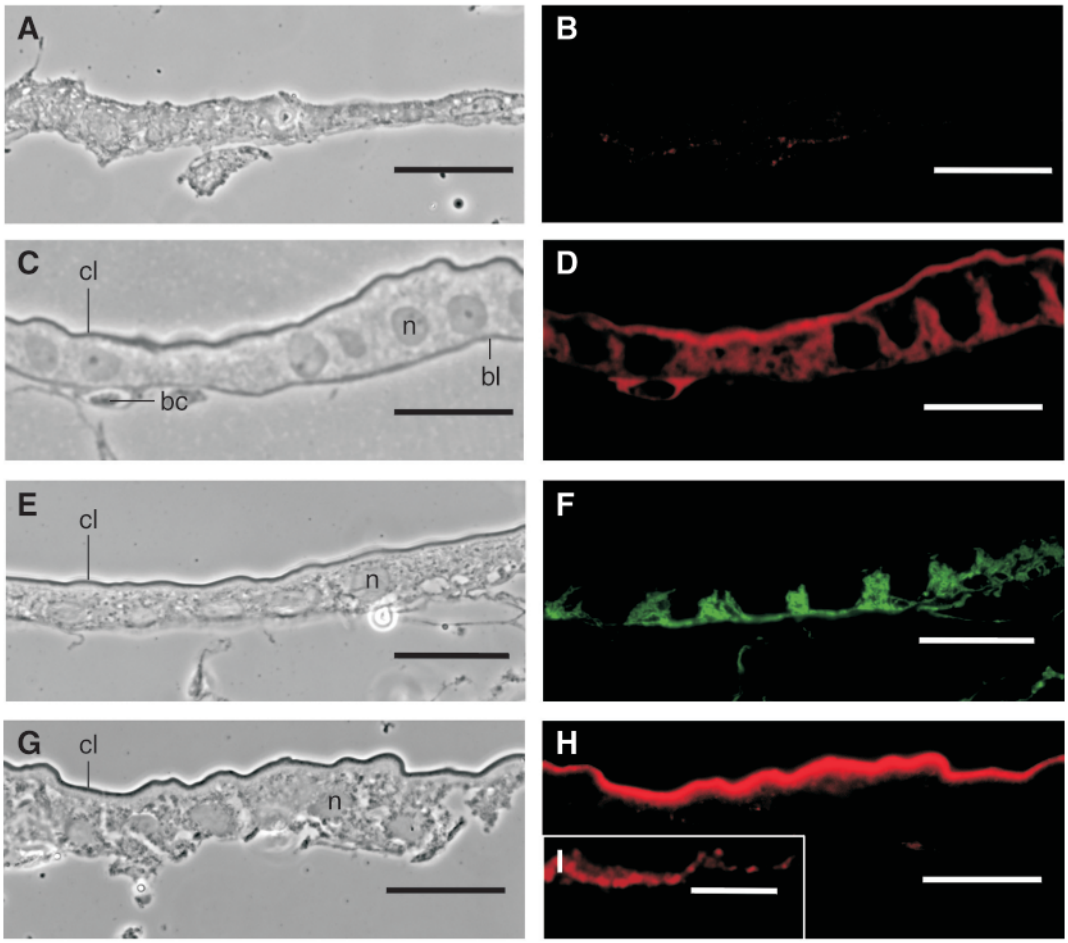

Fig. 5. Immunocytochemical localization of the V-type H^+-ATPase (A–D and G–I) and Na^+/K^+-ATPase (E,F). (A,C,E,G) Phase contrast and (B,D,F,H,I) fluorescence micrographs of 0.7 μm thick cryosections of the anterior sternal epithelium. (A,B) Control stage. (C–F) Stage of $CaCO_3$ deposit formation. (G–I) Stage of $CaCO_3$ deposit resorption. (I) Staining without amplification step. bc, blood cell; bl, basal lamina; cl, cuticle; n, nucleus. Scale bars, 25 μm (A–H); 16 μm (I).

Ultrastructural detection of portasomes

Since unspecific binding of the primary antibody to the cuticle cannot be excluded by western blot analysis we confirmed the presence of a VHA within the apical plasma membrane during the degradation of the $CaCO_3$ deposits using ultrastructural techniques. It is now generally accepted that the large cytoplasmic V_1 domain of the VHA can be visualized by transmission electron microscopy as 10 nm thick particles, the so-called portasomes (Wieczorek et al., 1999b). When the VHA occurs in high abundance portasomes can be recognized as membrane coats at the cytoplasmic side of the plasma membrane. We examined the ultrastructure of the ASE and PSE in high-pressure frozen and freeze-substituted sternal epithelial cells. Regions of the plasma membrane containing portasome coats were found in the apical membrane of the ASE (Fig. 6B–D) but not the PSE during the intramolt stage (three animals). No portasome coats were found at the apical or basolateral plasma membrane of the ASE and PSE during the control stage (three animals) or during $CaCO_3$ deposit formation (three animals).

Discussion

The present study reveals the contribution of a V-type H^+-ATPase (VHA) for epithelial proton transport in a crustacean calcifying epithelium. Expression analysis and immunocytochemistry of the VHA in Ca^{2+}-transporting and control stages correlates its function with mineralizing and demineralizing processes. We demonstrate for the first time a redistribution of the VHA from the basolateral to the apical plasma membrane within the same epithelial cells. This transition is consistent with a reversal of the direction of transepithelial proton transport between $CaCO_3$ deposit formation and resorption.

Expression of a V-type H^+-ATPase

The VHA is a large protein complex composed of two distinct domains: a cytoplasmic V_1 domain consisting of at least eight different subunits (A–H) and the integral membrane V_0 domain consisting of at least five subunits (a–d) (for a review, see Wieczorek et al., 2000). The B subunit is one of the two ATP binding subunits of the V_1 domain. Sequence

alignment of the cDNA-fragment with known sequences and immunocytochemical experiments indicate the expression of a VHA B-subunit and hence the expression of the VHA within the sternal epithelium of *Porcellio scaber*. The high identity of the deduced amino acid sequence with the corresponding crustacean and insect protein fragments is in accordance with the high evolutionary conservation of the VHA B-subunit (Novak et al., 1992). Since cuticle secretion is retarded in the anterior integument during the late premolt and intramolt stage, the ASE is specialized for the formation and degradation of the sternal $CaCO_3$ deposits (Ziegler, 1997b). Therefore, the increase in VHA expression within the ASE from the early premolt control stage to the calcium transporting stages during $CaCO_3$ deposit formation and $CaCO_3$ deposit resorption suggests a role of the VHA in the mineralization and demineralization processes, respectively. The PSE cells are involved in degradation of the old and formation of the new cuticle of the posterior sternites including demineralization and mineralization (Glötzner and Ziegler, 2000; Ziegler, 2002), but do not form $CaCO_3$ deposits. This implies that the rate of mineral transport by the PSE is smaller than in the ASE. Hence, the somewhat smaller expression of the VHA B-subunit within the PSE is in accordance with a role of the VHA in mineral deposition and resorption.

Subcellular localization of the V-type H^+-ATPase

The immunolocalization at the basolateral side of the epithelial cells in the late premolt stage corresponds well with the spatial distribution of the basolateral plasma membrane, which increases by an elaborate system of invaginations (Figs 5E,F and 6A), as shown previously using lanthanum as an extracellular marker and immunocytochemical localization of the Na^+/K^+-ATPase in the basolateral membrane (Ziegler, 1996, 1997a). Areas within the cytoplasm that do not include invaginations are virtually devoid of VHA. The strong increase in immunofluorescence near and within the cuticle of the epithelium from late premolt to intramolt indicates that the signal is mostly if not entirely due to a specific reaction of the

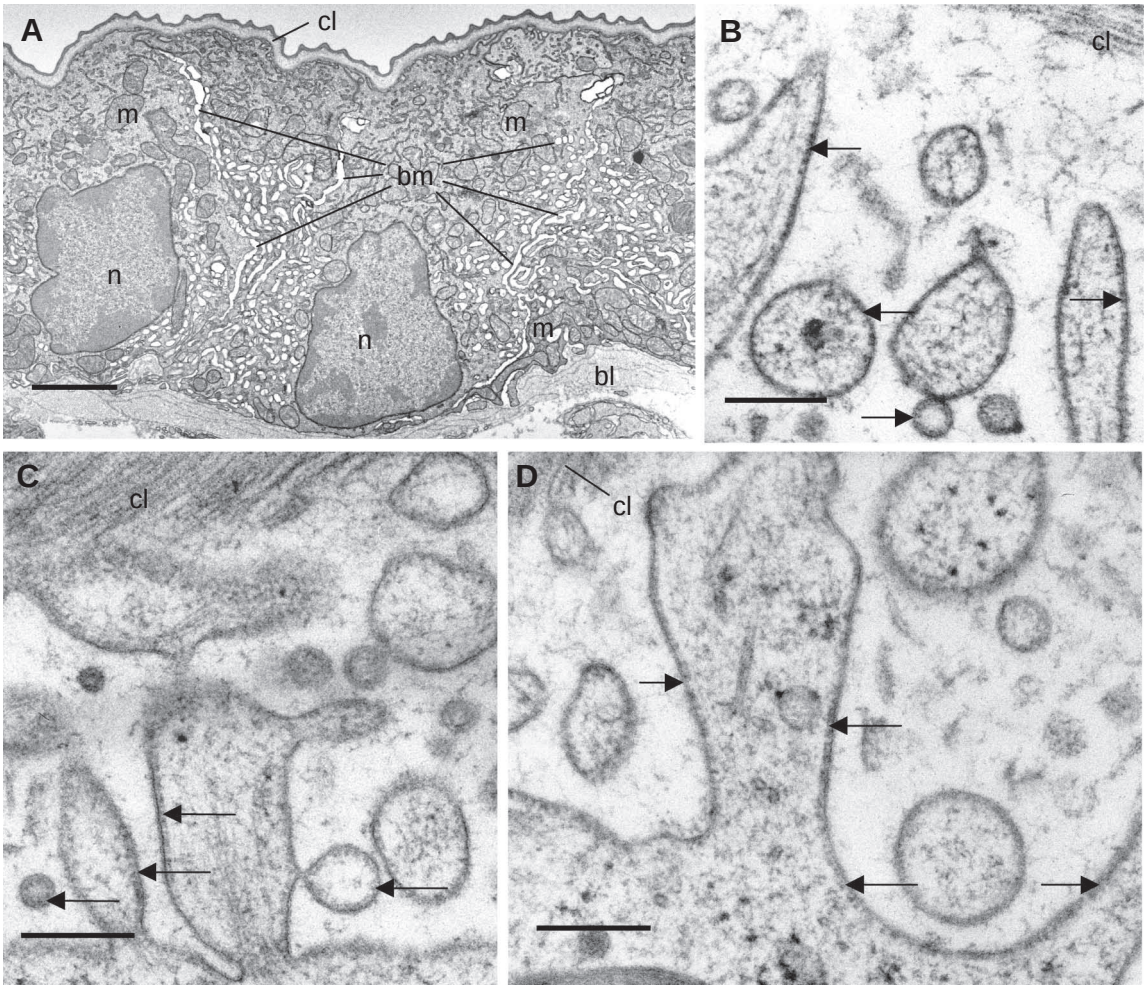

Fig. 6. Electron micrographs of the anterior sternal epithelium of *Porcellio scaber*. (A) Overview of chemically fixed epithelial cells during formation of the $CaCO_3$ deposits showing the distribution of the basolateral plasma membrane (bm) by extracellular invaginations. (B,C) Details of high-pressure frozen and freeze-substituted epithelial cells during the resorption of the $CaCO_3$ deposits showing portasome coats (arrows) at the apical plasma membrane. bl, basal lamina; cl, cuticle; m, mitochondrion; n, nucleus. Scale bars, 2 μm (A); 200 nm (B–D).

antibody to the VHA B-subunit. The ASE has numerous cellular projections of the epithelial cells, which extend into the new cuticle of the sternites (Ziegler, 1997b). The dot-like signal in specimens without an amplification of the immunoreaction suggests that the VHA is located within these projections. This is supported by coats of portasomes lining the apical plasma membranes of the ASE cells in the stage of $CaCO_3$ deposit resorption. The apparent lack of portasomes within the basolateral membrane, despite their immunolocalization during $CaCO_3$ deposit formation, may be explained by the failure of portasomes to form particle coats due to a lower portasome density. This may result from the larger surface of the basolateral plasma membrane as compared to the apical plasma membrane (Glötzner and Ziegler, 2000) and by a lower H^+ transport rate during the rather slow $CaCO_3$ deposit formation within 1 or 2 weeks as compared to their quick resorption within less than 24 h.

The increase in the VHA abundance from the control stage to the Ca^{2+}-transporting stages indicates a contribution of the VHA to the formation and degradation of $CaCO_3$ within the anterior sternites, in support of the results of the expression analysis. The results provide the first example of a function for the VHA in mineral deposition. The formation of the sternal deposits requires the transport of Ca^{2+} and HCO_3^- from the basal to the apical side of the epithelium and the release of protons during the formation of $CaCO_3$. These protons have to be transported back to the hemolymph to maintain electro-neutrality during the transport process and to avoid acidification of the liquid around the growing deposits. The high VHA expression and abundance within the basolateral membrane suggests a transcellular route for epithelial H^+-transport, with the VHA functioning in the extrusion of protons from the cytoplasm to the hemolymph. In most epithelial cells containing a VHA within the plasma membrane the protein complex is located apically (Wieczorek et al., 1999a). The presence of the VHA in the basolateral plasma membrane, however, is rare. To our knowledge this has been found only in vertebrate ocular ciliary epithelium (Wax et al., 1997) and in subpopulations of kidney intercalated B-cells. In the latter the VHA is localized either in the basolateral or apical plasma membranes depending on its presence in proton or bicarbonate secreting cells, respectively (Brown and Breton, 2000; Brown et al., 1988).

The most interesting result of the present study is the polarity reversal of VHA abundance in the ASE from the basolateral to the apical plasma membrane, correlating with the mineralization–demineralization cycle of the sternal $CaCO_3$ deposits. This reversal leads to a reduction of the VHA within the basolateral plasma membrane to virtually undetectable values, and to an increase of VHA abundance within the apical membrane. This polarity reversal correlates with the switch of the ASE cells from $CaCO_3$ secretion to $CaCO_3$ resorption. During the resorption of the $CaCO_3$ deposits protons must be transported from the hemolymph into the sternal exuvial gap to mobilize Ca^{2+} and HCO_3^- ions, which are then transported back to the hemolymph. A similar contribution to mineral resorption is known for a VHA in the apical plasma membrane of osteoclasts during bone resorption (Blair et al., 1989) and of the mantle epithelium of a freshwater clam during acid secretion to the shell (Hudson, 1993). The redirection of the VHA from the basolateral to the apical plasma membrane compartment within the same cell raises the question of the mechanism by which the sorting of the VHA switches between the opposite plasma membrane compartments. Expression analysis and the virtual lack of VHA within the cytoplasm favours a regulation by gene expression and retargeting to the appropriate plasma membrane compartment. The 2.8-fold increase of the apical plasma membrane surface area (Glötzner and Ziegler, 2000) from the stage of $CaCO_3$ deposit formation to $CaCO_3$ resorption is in accordance with a sorting of VHA containing intracellular vesicles to the target membrane. Such vesicles were reported from A-type intercalated cells of kidney collecting ducts, in which they regulate proton pumping by shuttling VHA molecules to and from the plasma membrane (for a review, see Brown and Breton, 1996).

Besides its function in proton transport a VHA functions in the energization of the plasma membrane by proton motive forces that mediate secondary transport processes by electric coupling (for a review, see Harvey and Wieczorek, 1997). This is the case in epithelia with little activity of the classical energizer of animal plasma membranes, the Na^+/K^+-ATPase, as in lepidopteran midgut (Jungreis and Vaughan, 1977; Wieczorek et al., 1999a) or malpighian tubules (Weng et al., 2003). In the ASE of *P. scaber* immunocytochemical localization of the Na^+/K^+-ATPase indicates a high abundance of the pump within the basolateral membrane (Ziegler, 1997a), arguing against an energization by the VHA. However, as pointed out by Wieczorek et al. (1999a), some epithelia energize the basolateral plasma membrane by the Na^+/K^+-ATPase and the apical membrane by a VHA. Therefore, besides a role of the VHA in H^+ extrusion, additional functions, possibly in facilitating Ca^{2+} influx or acid–base regulation, cannot be excluded.

We thank Dr D. Siebers for his generous support in initial experiments. This work was supported by the Deutsche Forschungsgemeinschaft (Zi 368/3-3) and the National Science Foundation (IBN-9807539).

References

Ahearn, G. A., Grover, M. L., Tsuji, R. T. and Clay, L. P. 1987). Proton-stimulated Cl-HCO_3 antiport by basolateral membrane vesicles of lobster hepatopancreas. *Am. J. Physiol.* **252**, R859-R870.

Ahearn, G. A., Mandal, P. K. and Mandal, A. (2001). Biology of the $2Na^+/1H^+$ antiporter in invertebrates. *J. Exp. Zool.* **289**, 232-244.

Altschul, S. F., Madden, T. L., Schaffer, A. A., Zhang, Z., Miller, W. and Lipman, D. J. (1997). Gapped BLAST and PSI-BLAST: a new generation of protein database search programs. *Nucleic Acid. Res.* **25**, 3389-3402.

Becker, A., Bismayer, U., Epple, M., Fabritius, H., Hasse, B., Shi, J. and Ziegler, A. (2002). Structural characterisation of X-ray amorphous calcium carbonate (ACC) in sternal deposits of the Crustacea *Porcellio scaber*. *Dalton. Trans.* **2003**, 551-555.

Blair, H. C., Teitelbaum, S. L., Ghiselli, R. and Gluck, S. (1989).

Osteoclastic bone resorption by a polarized vacuolar proton pump. *Science*. **245**, 855-857.

Brecevic, L and Nielson, A. E. (1989). Solubility of amorphous calcium carbonate. *J. Crystal Growth* **98**, 504-510.

Brown, D. and Breton, S. (1996). Mitochondria-rich, proton-secreting epithelial cells. *J. Exp. Biol.* **199**, 2345-2358.

Brown, D. and Breton, S. (2000). H^+V-ATPase-dependent luminal acidification in the kidney collecting duct and the epididymis/vas deferens: vesicle recycling and transcytotic pathways. *J. Exp. Biol*. **203**, 137-145.

Brown, D., Hirsch, S. and Gluck, S. (1988). An H^+-ATPase in opposite plasma membrane domains in kidney epithelial cell subpopulations. *Nature* **331**, 622-624.

Cameron, J. N. (1989). Post-moult calcification in the blue crab, *Callinectes sapidus*: timing and mechanism. *J. Exp. Biol.* **143**, 285-304.

Drobne, D. and Strus, J. (1996). Moult frequency of the isopod *Porcellio scaber*, as a measure of zinc-contaminated food. *Environ. Toxicol. Chem.* **15**, 126-130.

Finbow, M. E. and Harrison, M. A. (1997). The vacuolar H^+-ATPase: a universal proton pump pf eukaryotes. *Biochem. J.* **324**, 697-712.

Glötzner, J. and Ziegler, A. (2000). Morphometric analysis of the plasma membranes in the calcium transporting sternal epithelium of the terrestrial isopods *Ligia oceanica*, *Ligidium hypnorum* and *Porcellio scaber*. *Arthropod Struct. Dev*. **29**, 241-257.

Harvey, W. R. and Wieczorek, H. (1997). Animal plasma membrane energization by chemiosmotic H^+ V-ATPases. *J. Exp. Biol.* **200**, 203-216.

Hudson, R. L. (1993). Bafilomycin-sensitive acid secretion by mantle epithelium of the freshwater clam, *Unio complanatus*. *Am. Physiol. Soc*. **264**, R946-R951.

Jungreis, A. M. and Vaughan, G. L. (1977). Insensitivity of lepidopteran tissues to ouabain: absence of puabain binding and Na^+-K^+ ATPase in larval and adult midgut. *J. Insect. Physiol.* **23**, 503-509.

Laemmli, U. K. (1970). Cleavage of structural proteins during assembly of the head of bacteriophage T4. *Nature* **227**, 680-685.

Messner, B. (1965). Ein morphologisch-histologischer Beitrag zur Häutung von *Porcellio scaber* latr. und *Oniscus asellus* l. (Isopoda terrestria). *Crustaceana* **9**, 285-301.

Novak, F. J. S., Gräf, R., Waring, R. B., Wolfersberger, M. G., Wieczorek, H. and Harvey, W. R. (1992). Primary structure of V-ATPase subunit B from *Manduca sexta* midgut. *Biochim. Biophys. Acta* **1132**, 67-71.

Onken, H. and Putzenlechner, M. (1995). A V-ATPase drives active, electogenic and Na^+-independent Cl^- absorption across the gills of *Eriocheir sinensis*. *J. Exp. Biol.* **198**, 767-774.

Sanger, F., Nicklen, S. and Coulson, A. R. (1977). DNA sequencing with chain terminating inhibitors. *Proc. Natl. Acad. Sci. USA* **74**, 5463-5467.

Steel, C. G. H. (1993). Storage and translocation of integumentary calcium during the moult cycle of the terrestrial isopod *Oniscus asellus* (L.). *Can. J. Zool*. **71**, 4-10.

Towle, D. W., Rushton, M. E., Heidysch, D., Magnani, J. J., Rose, M. J., Amstutz, A., Jordan, M. K., Shearer, D. W. and Wu, W.-S. (1997). Sodium/proton antiporter in the euryhaline crab *Carcinus maenas*: molecular cloning, expression and tissue distribution. *J. Exp. Biol.* **200**, 1003-1014.

Walther, P. and Ziegler, A. (2002). Freeze substitution of high-pressure frozen samples: the visibility of biological membraneas is improved when the substitution medium contains water. *J. Microsc.* **208**, 3-10.

Wax, M. B., Saito, I., Tenkova, T., Krupin, T., Becker, B., Nelson, N., Brown, D. and Gluck, S. L. (1997). Vacuolar H^+-ATPase in ocular ciliary epithelium. *Cell Biol.* **94**, 6752-6757.

Weihrauch, D., Ziegler, A., Siebers, D. and Towle, D. W. (2001). Molecular characterization of V-type H^+-ATPase (B-subunit) in gills of euryhaline crabs and its physiological role in osmoregulatory ion updake. *J. Exp. Biol.* **204**, 25-37.

Weihrauch, D., Ziegler, A., Siebers, D. and Towle, D. W. (2002). Active ammonia excretion across the gills of the green shore crab *Carcinus maenas*: participation of Na^+/K^+-ATPase, V-type H^+-ATPase and functional microtubules. *J. Exp. Biol.* **205**, 2765-2775.

Weng, X.-H., Huss, M., Wieczorek, H. and Beyenbach, K. W. (2003). The V-type H^+-ATPase in Malpighian tubules of *Aedes aegypti*: localization and activity. *J. Exp. Biol.* **206**, 2211-2219.

Wieczorek, H., Brown, D., Grinstein, S., Ehrenfeld, J. and Harvey, W. R. (1999a). Animal plasma membrane energization by proton-motive V-ATPases. *BioEssays* **21**, 637-648.

Wieczorek, H., Grüber, G., Harvey, W. R., Huss, M. and Merzendorfer, H. (1999b). The plasma membrane H^+-V-ATPase from tobacco hornworm midgut. *J. Bioenerg. Biomem.* **31**, 67-75.

Wieczorek, H., Grüber, G., Harvey, W. R., Huss, M., Merzendorfer, H. and Zeiske, W. (2000). Structure and regulation of insect plasma membrane H^+ V-ATPase. *J. Exp. Biol.* **203**, 127-135.

Wieser, W. (1964). Über die Häutung von *Porcellio scaber* Latr. *Verh. Dtsch. Zool. Ges.* **1964**, 178-195.

Zare, S. and Greenaway, P. (1998). The effect of moulting and sodium depletion on sodium transport and the activities of Na^+K^+-ATPase, and V-ATPase in the freshwater crayfish *Cherax destructor* (crustacea: parastacidae). *Comp. Biochem. Physiol.* **119A**, 739-745.

Ziegler, A. (1994). Ultrastructure and electron spectroscopic diffraction analysis of the sternal calcium deposits of *Porcellio scaber* Latr. (Isopoda, Crustacea). *J. Struct. Biol.* **112**, 110-116.

Ziegler, A. (1996). Ultrastructural evidence for transepithelial calcium transport in the anterior sternal epithelium of the terrestrial isopod *Porcellio scaber* (Crustacea) during the formation and resorption of $CaCO_3$ deposits. *Cell. Tissue. Res.* **284**, 459-466.

Ziegler, A. (1997a). Immunocytochemical localization of Na^+,K^+-ATPase in the calcium-transporting sternal epithelium of the terrestrial isopod *Porcellio scaber* Latr. (Crustacea). *J. Histochem. Cytochem.* **45**, 437-446.

Ziegler, A. (1997b). Ultrastructural changes of the anterior and posterior sternal integument of the terrestrial isopod *Porcellio scaber* Latr. (Crustacea) during the moult cycle. *Tissue Cell* **29**, 63-76.

Ziegler, A. (2002). X-ray microprobe analysis of epithelial calcium transport. *Cell Calcium* **31**, 307-321.

Ziegler, A. and Merz, E. (1999). Membrane particle distribution in the sternal epithelia of the terrestrial isopod *Porcellio scaber* Latr. (Crustacea, Oniscidea) during $CaCO_3$ deposit formation and resorption, a freeze-etch analysis. *J. Struct. Biol.* **127**, 263-278.

Ziegler, A., Weihrauch, D., Towle, D. W. and Hagedorn, M. (2002). Expression of Ca^{2+}-ATPase and Na^+/Ca^{2+}-exchanger is upregulated during epithelial Ca^{2+} transport in hypodermal cells of the isopod *Porcellio scaber*. *Cell Calcium* **32**, 131-141.